

# NUMERICAL STUDY ON FATIGUE NOTCH SENSITIVITY OF HIGH AND MIDDLE STRENGTH CARBON STEELS FOR WELDED STRUCTURES

Seiichiro TSUTSUMI<sup>1</sup>, Ayang BUERLIHAN<sup>2</sup> and Riccardo FINCATO<sup>3</sup>

<sup>1</sup>Member of JSCE, Associate Professor, Joining and Welding Research institute, Osaka University  
(11-1, Mihogaoka, Ibaraki, Osaka, 567-0047, Japan)

E-mail: [tsutsumi@jwri.osaka-u.ac.jp](mailto:tsutsumi@jwri.osaka-u.ac.jp) (Corresponding Author)

<sup>2</sup>Member of JSCE, Joining and Welding Research institute, Osaka University  
(11-1, Mihogaoka, Ibaraki, Osaka, 567-0047, Japan)

E-mail: [ayang@jwri.osaka-u.ac.jp](mailto:ayang@jwri.osaka-u.ac.jp)

<sup>3</sup>Member of JSCE, Joining and Welding Research institute, Osaka University  
(11-1, Mihogaoka, Ibaraki, Osaka, 567-0047, Japan)

E-mail: [fincato@jwri.osaka-u.ac.jp](mailto:fincato@jwri.osaka-u.ac.jp)

The purpose of this study is to investigate the effect of notches on fatigue strength of middle (i.e., SM490) and high (i.e., HT780) strength steels. The study is based on finite element analyses on two types of notched specimens referring to an experimental work found in the literature. A novel approach is proposed to characterize the fatigue performance of the samples based on elasto-plastic analyses carried out with an unconventional plasticity model, the Fatigue SS model, proposed by the authors. The fatigue life, expressed as the sum of crack initiation life and crack propagation life, was predicted under unidirectional cyclic loading conditions ( $R = 0$ ). The main advantages of the novel methodology consist in considering the effect of irreversible deformations and the effect of the local geometry on the initiation and propagation of the crack. The numerical results were validated against experimental data proving the reliability of the new assessment method.

**Key Words :** *Fatigue crack initiation, fatigue crack propagation, elastoplasticity, finite element analyses.*

## 1. INTRODUCTION

Most of the steel structures in service have notched components that play a fundamental role in crack formation and propagation when structures are subjected to cyclic loading. In fact, the presence of notches may induce high-stress concentration in local areas. Consequently, even if the magnitude of the nominal stress is lower than the macroscopic yield stress, local yielding might occur around a notch. The accumulation of irreversible strain under cyclic loading, progressively induces fatigue cracks to initiate and to grow. On the other side, the cyclic stress-strain responses vary depending on the shape of notches and the mechanical properties of the material. Thus, different crack initiation and propagation behaviors are functions of the local stress field, material response (i.e., nonlinear behavior) and geometry.

In the engineering practice, the design of metallic

structures and components is commonly based on linear fracture mechanics, assuming an elastic response of the material, adopting S-N diagrams and stress intensity factor  $K$  to evaluate the fatigue failure. In particular, crack propagation is often estimated by using the well-known Paris' law<sup>1)</sup> that relates the crack growth rate  $da/dN$  with the range of stress intensity  $\Delta K$  by means of material constants. This approach can give a reliable estimation of the fatigue performance, however, it neglects the contribution of plastic strain and therefore results less accurate in case of strong material nonlinearities or nonlinearities derived from the loading history<sup>2)-4)</sup>.

Alternatively, in case of material plasticization, the  $J$ -integral<sup>5)</sup> or cyclic  $J$ -integral<sup>6)</sup> (i.e.,  $\Delta J$ ) approaches are often adopted. These methods can be used in both large-scale yielding (LYS) and in small-scale yielding (SSY) problems, however, the influence of the local geometry at the crack tip might not

be accurate since they express an averaged strain release rate, which depends on the choice of the integration contour surrounding the crack. Other limitations are pointed out in<sup>7), 8)</sup>.

In addition to the aforementioned shortcomings, another issue lies on the correct evaluation of the material plasticization that leads to the crack initiation and influences the following propagation. Phenomenological models conventionally consider the stress space divided into elastic and plastic domains, allowing the generation of inelastic strain only when the stress state lies on the macroscopic yield surface during loading. Recently, the authors developed an elastoplastic model<sup>9)</sup> (i.e., Fatigue SS), based on an unconventional approach, capable of describing a non-linear response of the material even for stress states lower than the macroscopic yield stress. This aspect makes the Fatigue SS model suitable for the description of material deformation in cyclic mobility problems and low/high cycle fatigue problems<sup>10)-12)</sup>.

Miki *et al.*<sup>13)</sup> conducted an experimental campaign to investigate the effect of the notch geometry and plastic strain on the fatigue strength. Several samples, with different notch shapes, were subjected to fully reversed ( $R = -1$ ) and unidirectional cyclic loading ( $R = 0$ ) conditions. In addition, the experiments considered two separate materials: a middle (i.e., SM490) and high (i.e., HT780) strength steels. The influence of notches on fatigue strength was studied and the relations between crack initiation fatigue life and total strain range was given. However, one problematic aspect was represented by the detection of minute fatigue cracks at the notch roots, therefore, the crack initiation life was defined when a crack of length of 0.5mm was discovered on the surface of the specimen. Moreover, even if the experiments characterized the different fatigue performance of the steels against the notch geometries (i.e., for different stress intensity factors) the mechanism for the crack propagation and the influencing factors were not fully investigated. Therefore, the aim of the present work is the clarification of the effect of notch sensitivity on both crack initiation and propagation for steels with different strengths.

In this study, the crack initiation and propagation life were investigated by means of finite element analyses (i.e., FEA), considering two notch geometries (i.e., type-4 and type-5 samples in Miki *et al.*<sup>13)</sup>) and two steels, SM490 and HT780 respectively. Moreover, a novel approach for the characterization of the fatigue life is presented. In detail, the crack initiation life  $N_c$  is investigated by means of the Fatigue SS model, whereas the crack propagation life  $N_p$  has been modeled as a series of fatigue cracks, similarly to previous works of the authors<sup>14), 15)</sup>. The advantage

of the proposed methodology consists in the possibility of considering the local geometry in the surrounding of the crack tip as well as the influence of the non-linear material response on the stress field. The work is organized as follows. Section 2 describes the numerical approach in terms of main features of the Fatigue SS model and the crack initiation and propagation criteria. Section 3 presents the numerical modeling of the samples. A discussion of the results of the FEA against the experimental data is proposed in sections 4 and 5. Lastly, section 6 summarizes the main findings and the future studies.

## 2. FATIGUE LIFE EVALUATION

The benefit of FEA lies on the possibility of reducing the costs of experimental campaigns and the possibility of conducting simulations and parametric study (i.e., changes of geometry, materials, loading conditions) in relatively short time. On the other hand, the accuracy of the results is strongly connected with the modeling assumptions (i.e., mesh, element type, boundary conditions, etc.) and the constitutive modeling of the mechanical response of the material (i.e., linear elasticity, elastoplasticity, etc.). As mentioned in the introduction, in case of LYS the adoption of linear elastic fracture mechanics (LEFM) cannot give reliable results in term of fatigue. A more appropriate approach consists in adopting an elastoplastic constitutive model and to consider the effect of irreversible strain on crack initiation and propagation (i.e., elastic-plastic fracture mechanics EPFM). The second strategy is adopted in this work.

### (1) The Fatigue SS model

Experimental evidence showed a progressive plasticization in metallic materials subjected to cyclic loading with nominal stress ranges within the elastic domain<sup>17), 18)</sup>. This phenomenon is due to the presence of material defects, for instance inclusions and micro voids, that induce an alteration of the stress field in the material with consequent plasticization. A proper description of material rheology should be carried out with micro or meso-scale models<sup>19)</sup>, since a phenomenological approach cannot account for single local material inhomogeneities.

Recently, the authors developed a phenomenological elastoplastic constitutive model capable to account for plastic strain generation even for stress states lower than the macroscopic yield stress<sup>9), 16)</sup>. The main idea is to introduce an isotropic scalar damage-like variable to the constitutive equation of an unconventional plasticity theory, the subloading surface theory<sup>20), 22)</sup>. The damage variable considers the progressive accumulation of material defects with the evolution of plastic accumulation, contributing to the

opening of hysteresis loops and the description of material softening. The definition of the evolution of the damage-like variable depends on plastic deformation, however, it has no effect on the elastic stiffness and on the plastic flow (i.e., uncoupled variable). It should be highlighted that, due to the scale of observation, the progressive damaging is described as averaged and homogeneous process without considering single defects. However, this phenomenological description reproduced well metals behavior under low or high cycle fatigue conditions<sup>9)-12)</sup>.

A description of the constitutive equations of the Fatigue SS model is here omitted. Details on the Fatigue SS model can be found in<sup>9)</sup>.

## (2) Crack initiation criterion $N_c$

Estimation of crack initiation life  $N_c$  can be carried out following several approaches grouped into two main categories: stress-strain approaches and local approaches based on continuum damage mechanics (CDM). The present study follows the first category, as in previous works of the authors<sup>10), 11)</sup>, relating the total strain range with the number of cycles for the crack opening. This approach is known to predict well the fatigue performance under constant amplitude loading conditions<sup>23)-25)</sup>.

In particular, the choice is motivated by the adoption of the Fatigue SS model, that allows to describe realistically the material ratcheting and the opening and following saturation of the hysteresis loop size. Conventional plasticity theories cannot give an accurate result of the material ratcheting since they cannot predict a smooth transition between the elastic and plastic domain and therefore an adequate description of hysteresis loops size. The relationship between crack initiation life  $N_c$  and total strain range  $\Delta\varepsilon$  is reported in the following equations Eq. (1) and Eq. (2) for the SM490 and HT780 steels, respectively, and graphically displayed in Fig. 1.

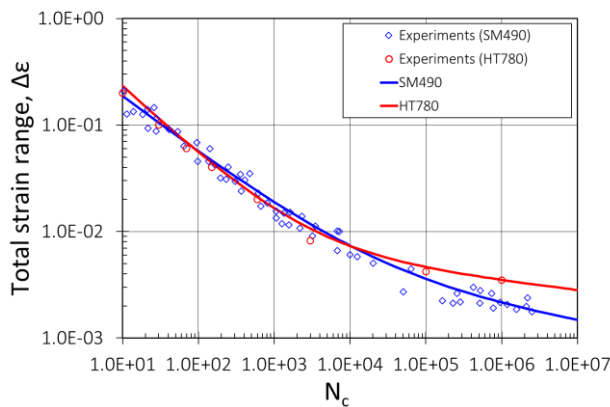


**Fig. 1** Fatigue crack initiation criteria.

$$\Delta\varepsilon = 0.625N_c^{-0.541} + 0.0091N_c^{-0.117} \quad (1)$$

$$\Delta\varepsilon = 1.029N_c^{-0.665} + 0.0112N_c^{-0.086} \quad (2)$$

The two equations are modified forms of the empirical approach proposed in<sup>23), 26)</sup>, where the coefficients for the multipliers and the exponents were calibrated to reproduce the material behaviors reported in the fatigue experiments in<sup>13), 26), 27)</sup>. Same approach was adopted in previous works of the authors<sup>14), 15)</sup>. As it can be seen in Fig. 1 the two solid lines have a different trend, especially in the high cycle regime, where the high strength steel is characterized by a better fatigue performance. From a computational point of view, the values of the total strain range  $\Delta\varepsilon$  are obtained from the element displaying the highest cumulative plastic strain.

Moreover, the previous relationships do not consider the effect of the mean stress  $\sigma_m$ , even under the applied unidirectional cyclic loading conditions. In fact, observing the hysteresis loops, the effect of the mean stress in correspondence of the notch tends to be negligible.

## (3) Crack propagation criterion $N_p$

As mentioned in the introduction, the main idea is to evaluate the crack propagation as a series of fatigue cracks that progressively open depending on the elastoplastic behavior of the material. The benefit of this approach consists in a criterion capable of accounting for irreversible deformations and for the local shape at the crack tip, aspects that are neglected in the conventional LEFM and with the adoption of the cyclic J-integral approach.

In detail, the crack growth rate is evaluated by means of the following Eq. (3):

$$\frac{da}{dN} = \frac{\Delta a}{N_c} \quad (3).$$

The  $N_c$  term is evaluated by means of the total strain range, obtained from the local stabilized hysteresis loops in the elastoplastic analyses. The total strain range is extrapolated from the local element showing the highest plastic accumulation which is located in correspondence of the crack tip under the effect of the stress concentration. The term  $\Delta a$  represents the increment of crack length associated with the corresponding crack initiation  $N_c$ . The crack propagation is therefore imagined as a progressive opening of  $\Delta a$  lengths depending on the number of cycles for the crack to initiate and it is a function of the local geometry and stress field.

From a theoretical point of view the increment of crack length should be a variable depending on the mechanical properties of the material and on the mesh used in the numerical modeling (i.e., element size and element type). In a previous work<sup>15)</sup>, the authors conducted a parametric study on a SM490 steel CT specimen in order to characterize the crack increment under cyclic loading conditions ( $R = 0.1$ ). It was shown that the experimental crack growth rate can be numerically reproduced imposing a constant value on

$\Delta a$  that depends on the element size. Moreover, an analytical relationship to define the value of the crack increment  $\Delta a$  as a function of the element size was proposed. In this study  $\Delta a = 5\mu m$  was chosen based on<sup>15</sup>.

#### (4) Fatigue life $N_f$

The total fatigue life for the specimens is obtained by adding the crack initiation life  $N_c$ , described in subsection 2-(2), together with the crack propagation life  $N_p$ , obtained with the methodology described in subsection 2-(3) (i.e.,  $N_f = N_c + N_p$ ).

A schematic flow chart for the computation of the total fatigue life is reported in Fig. 2.

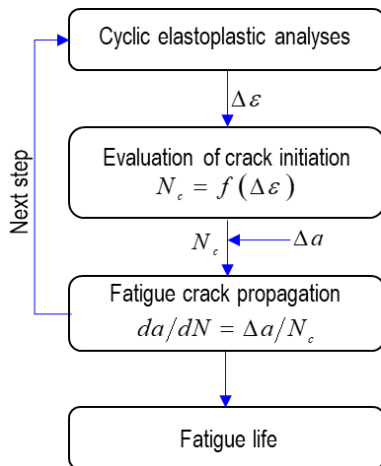


Fig. 2 Flow chart for the computation of  $N_f$ .

### 3. NUMERICAL MODELING

Finite element (FE) models were generated based on two of the geometries of the fatigue test specimens proposed by Miki<sup>28</sup>) (i.e., Type-4 and Type-5), here renamed Model-O and Model-U according to the shape of the notch (see Fig. 3). In order to reduce the computational effort and due to the shape of the samples, only 1/4 of the geometry was modeled in 3D imposing isostatic boundary conditions. Linear 8-node hexahedral elements (i.e., C3D8 Abaqus elements) were used in the simulations. Different mesh discretizations were adopted with denser meshes (minimum element size of  $50\mu m$ ) in the surrounding of the notches and coarser meshes in the remaining parts, where elastic deformations are expected.

The Fatigue SS model was implemented via user subroutine for the commercial code Abaqus (ver. 6.14-4) and used to describe the nonlinear material behavior of SM490 and HT780 steels. The SM490 and HT780 material parameters for the Fatigue SS model were calibrated against monotonic tensile and cyclic loading tests in<sup>14), 15)</sup>. The analyses were conducted with stress ranges of 150, 300, 500MPa, and with a stress ratio of  $R=0$  in each model (see the sketch of the amplitude in Fig. 4).

Besides, to evaluate the effect of the shape of the notch on stress concentration, elastic analyses were carried out and stress concentration factors were compared with the values reported in<sup>13)</sup> (see Table 1). The numerical error is quite limited with a slight overestimation in case of Model-U.

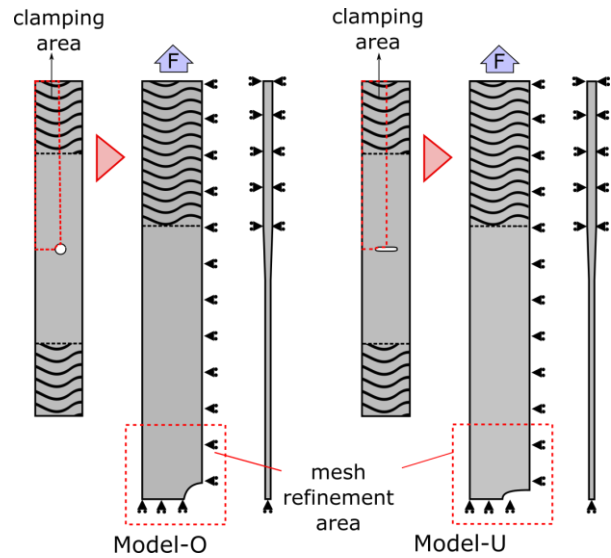


Fig. 3 Sketch of the geometry and boundary conditions for Model-O and Model-U.

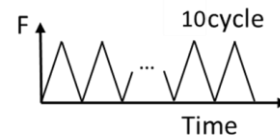


Fig. 4 Sketch of the unidirectional loading conditions.

Table 1 Stress concentration factors  $K_t$ .

	$K_t$ numerical	$K_t$ (Miki <i>et al.</i> <sup>13)</sup> )	Error [%]
Model-O	2.447	2.45	0.12
Model-U	4.843	4.55	6.43

### 4. RESULTS

This section reports the results obtained in the numerical simulations. Firstly, the effect of the stress concentration factor in relation with the material and notch geometry will be discussed. The fatigue results are then compared with the experimental data and finally some numerical consideration on the crack initiation and propagation are presented.

The evaluation of crack initiation life was based on the total strain range obtained at the 10th loading cycle since the hysteresis loops size tends to stabilize in both notched configurations and for both type of steels. An example of the evolution of the total strain ranges for the 500 MPa cyclic loading condition and for different crack lengths is reported in Fig. 5. As it can be seen, after an initial increment due to the material hardening, the strain ranges seem to saturate. The difference in magnitude of  $\Delta \epsilon$  between Model-O and Model-U seems more marked in the HT780 steel.

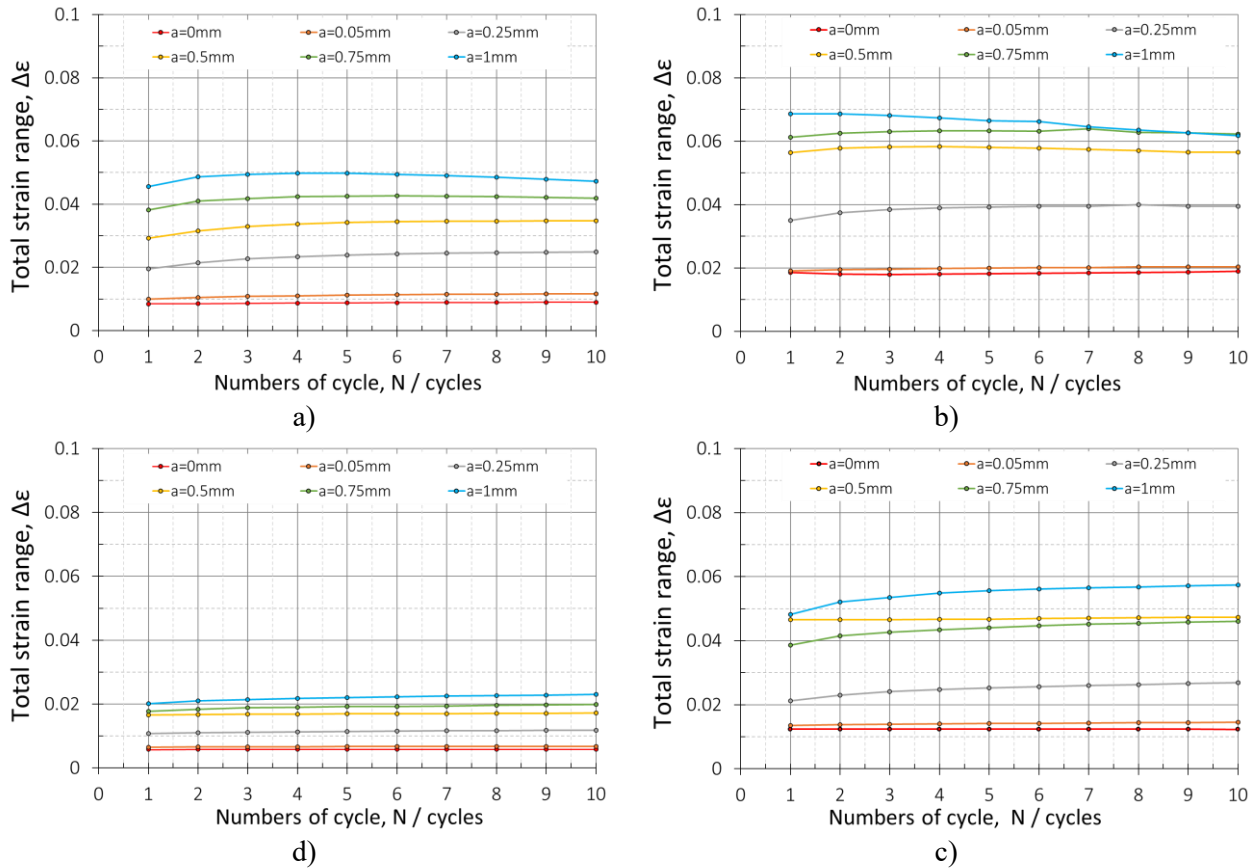


Fig. 5 Total strain for the 500 MPa. SM490 steel: a) Model-O, b) Model-U. HT780 steel: c) Model-O, d) Model-U.

### (1) Stress concentration vs fatigue life.

Fig. 6 reports the crack growth rate computed with Eq. (3) at different values of the crack length. With the progression of the crack, the growth rate shows a monotonic increase with a progressive saturation for higher values of  $a$ . In addition, the growth rate is higher in case of a U-shaped notch due to the higher stress concentration and the consequent higher magnitude of plastic strain affecting  $N_c$ . The SM490 steel in Model-U gives the highest crack growth rate. It should be reminded that, since the crack increment  $\Delta a$  is constant, the speed is governed uniquely by the number of cycles to crack initiation that are inversely proportional to the total strain range.

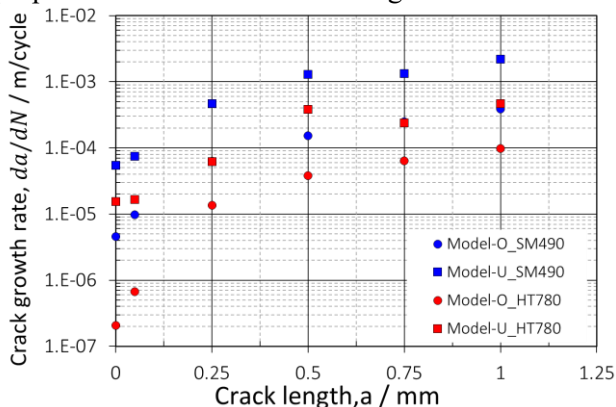


Fig. 6 Crack growth rate against crack length for the two steels and notches ( $\Delta\sigma = 300MPa$ ).

The more the material is prone to generate plastic deformation, the lower is the number of cycles to form the subsequent crack. This aspect can be observed in the graph of Fig. 7, where the crack length is reported against the total fatigue life (i.e., number of cycles to failure). Higher values of the stress concentration factor, obtained in Model-U (squared markers), imply a shorter fatigue life. Moreover, under the same notch configuration, the fatigue life depends on the mechanical properties of the material, giving a better performance for the 'stiffer' material. Comparing the fatigue lives of the SM490 and HT780 steels it is possible to see that the notch geometry has more relevance in the high strength steel compared with the middle strength one.

In fact, the gap in number of cycles between the red markers, at 1mm crack lengths, is 12 times larger compared with the blue markers.

Fig. 8 displays the stress at  $2 \times 10^6$  cycles against the stress concentration factors. The blue markers are representative of the SM490 steel whereas the red markers indicate the HT780 steel results. Black 'x' markers indicate the experimental results obtained by Miki<sup>(28)</sup>. As it can be seen, the numerical analyses agree sufficiently well with the experimental results, catching the decreasing trend of fatigue life with the increase of stress concentration factor. Moreover, it should be highlighted that for lower values of  $K_t$  the

mechanical properties of the material play a fundamental role in the fatigue performance (i.e., at  $K_t = 2.55$  the difference between the two steels is 138 MPa), whereas the difference between the SM490 and HT780 steels tends to diminish (i.e., at  $K_t = 4.85$  the difference between the two steels is 83 MPa) with the increase of the stress concentration factor. The higher transition in stress from  $K_t = 2.55$  to  $K_t = 4.85$  is observed for the HT780 steel with a 164 MPa decrease, while the SM490 shows 100 MPa decrease.

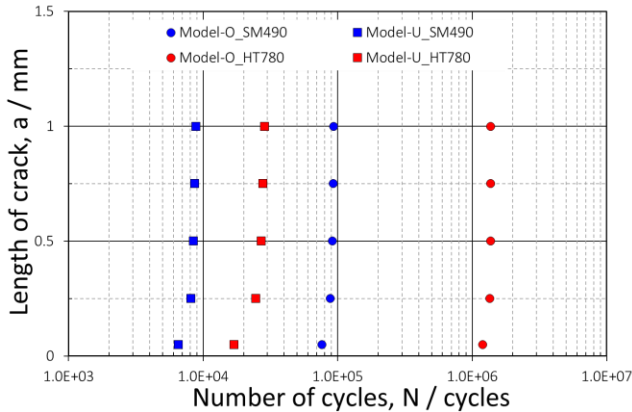


Fig. 7 Crack length against number of cycles for the two steels and notches ( $\Delta\sigma = 300\text{MPa}$ ).

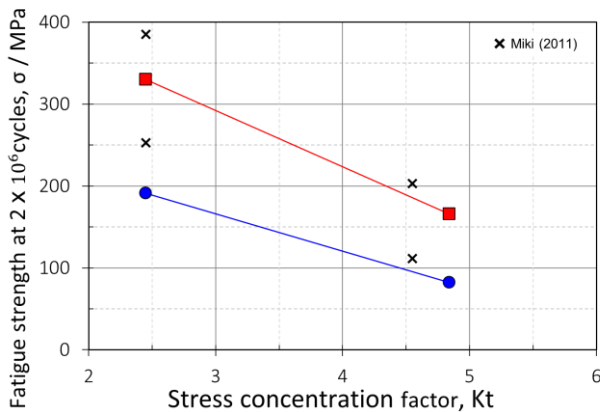


Fig. 8 Fatigue strength at  $2 \times 10^6$  cycles vs stress concentration factor.

## (2) Numerical and experimental S-N data.

This section presents the results of numerical fatigue simulations against experimental data (see Fig. 9). The numerical results are reported with squared and circular markers for the Model-U and Model-O, respectively. The blue color is associated with the SM490 steel whereas the red color represents the HT780 steel. Hollow and solid black markers report the fatigue experimental data obtained by Miki<sup>28)</sup>. As it can be seen the proposed approach seems to agree well with the experimental data, especially for high nominal stress regime, while some discrepancies can be found in the lower nominal stress regime.

In order to verify the validity of the proposed methodology, the numerical and experimental data are reported in the different visualization of Fig. 10. Here, the experimental and numerical stress amplitude are

reported at the experimental number of cycles to failure. It should be mentioned that, while the experimental data were reported directly from the reference<sup>28)</sup>, the additional numerical data were obtained by means of a linear interpolation between the computed points since the experimental and numerical loading conditions slightly differ.

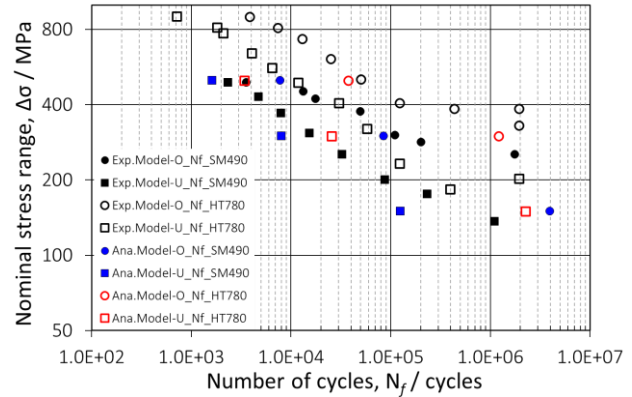


Fig. 9 S-N<sub>f</sub> data for Model-O, Model-U and the two steels.

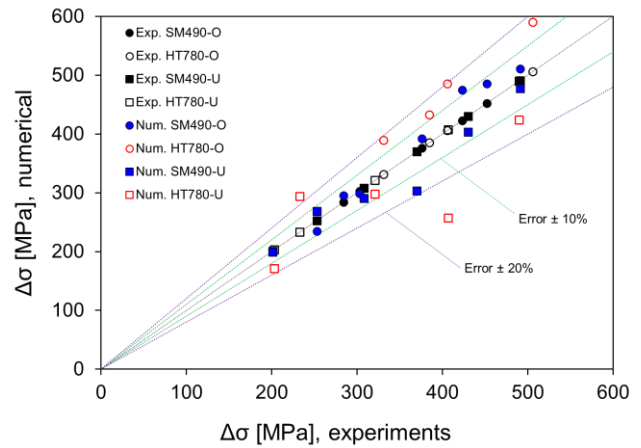


Fig. 10 Experimental vs numerical predicted stress amplitude for the experimental number of cycles at failure.

The error in the FEA is represented by the distance of the red and blue points from the diagonal (i.e., the experimental counterpart). Additionally, the graph reports green and purple dashed lines, indicating errors of 10% and 20% respect to the experiments. As it can be seen, all the simulations lie within 20% error, except for two points for Model-U and HT780 steel. In general, the error committed in the SM490 steel results lower than the one obtained for the HT780 steel. One possible explanation might be the choice of the value for crack increment  $\Delta a$  adopted in the crack propagation evaluation. The value of  $5 \mu\text{m}$  has been in fact obtained through numerical simulation carried out on a CT SM490 specimens and therefore might not be accurate to represents a material with different mechanical properties. Future works will investigate this aspect. Overall, it can be concluded that the proposed methodology can catch well the fatigue failure of the investigated samples.

### (3) Numerical comparison between $N_c$ and $N_p$ .

The current subsection analyses the numerical results comparing the crack initiation against the crack propagation life. Fig. 11 graphically reports the results. The solid bars (blue and red) indicate  $N_c$  whereas  $N_p$  is displayed with striped bars. The sum of the two contributions from the 100% of the fatigue life.

In general, the number of cycles for crack formation seems dominant independently from the material and the notch geometry. In particular Fig. 11a and c refer to the Model-O fatigue performance for SM490 and HT780 steels, respectively. On the other hand, Fig. 11b and d display the analyses for Model-U. In particular,  $N_c$  in Model-O shows a decreasing tendency with the increase of the loading condition in both materials, accounting for more than 80% of the total fatigue life in four of the six cases. The minimum  $N_c$  is obtained for the HT780 steel and  $\Delta\sigma = 500\text{MPa}$  ( $N_c \sim 70\%$ ). In Model-U the decrease of the fatigue life with the applied loading conditions is less evident and the crack propagation life assumes a more important role. This aspect is due to the higher stress field at the notch (i.e., higher stress concentration factor) inducing the development of plastic deformations and therefore larger hysteresis loops, shortening the  $N_c$  term without cracks and for the

cracks opening during the propagation. The minimum  $N_c$  is obtained for the HT780 steel under 300 or 500 MPa nominal loading condition.

A comparison with the experimental data in Miki *et al.*<sup>13)</sup> is not available, since the results on crack initiation and propagation life are not reported for the two specimens selected. However, the numerical simulations seem to provide a similar ratio between the number of cycles to crack initiation and propagation to the specimen with different notch shape reported in<sup>13)</sup>.

## 5. DISCUSSION

As reminded in the introduction the benefit of the proposed methodology lies in the possibility of accounting for inelastic strains as well as the local geometrical effect at the crack tip, influencing the stress field and therefore the crack propagation. An approach based on LEFM seems not suitable for the application to LYS problems, whereas the use of the *cyclic J-integral* is less accurate in taking into account the effect of the local geometry in the surrounding of the crack tip since the accuracy depends on the choice of the integration contour surrounding the crack. However, some issues connected with the fatigue life investigations still remain unclear even with the proposed methodology.

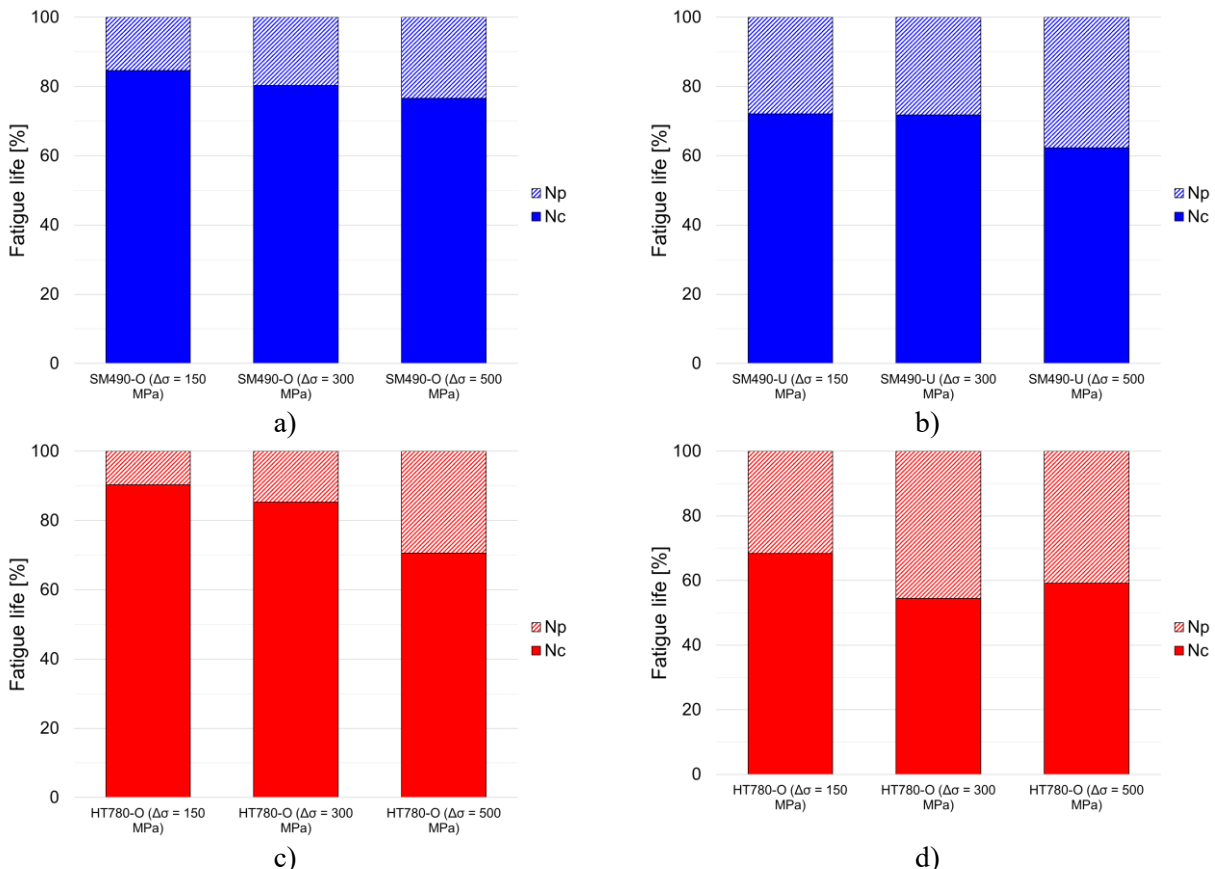


**Fig. 11** Numerical comparison between crack initiation and crack propagation life. Model-O: a) SM490 and c) HT780 steels. Model-U: b) SM490 and d) HT780 steels.

- The life prediction under various and especially multiaxial loading conditions has not been investigated yet with the novel approach, and it remains an open topic on the applicability of the proposed methodology to general cases.
- The analyses were conducted on 3D samples; however, the crack propagation has been investigated by adopting a circular crack, without a differentiation on the direction of the crack front evolution. Future works will investigate this aspect.
- The calibration of the crack increment  $\Delta a$  was conducted only on SM490, leading to less precise computation in case of high strength steel. Moreover, the definition of  $\Delta a$  is based on a crack propagation on a CT specimen considering only mode I for the crack.
- The methodology has been applied on virgin material, the validation of the approach in case of welded material is left to future works.

## 6. CONCLUSIONS

The present work aimed to clarify the mechanism of crack initiation and propagation in relation to the notch sensitivity. Two different materials, a middle and high strength steels were considered, together with two notch geometries, reproducing the experimental results carried out by<sup>13), 28)</sup>. Moreover, a novel methodology for the evaluation of the fatigue performance is introduced, aiming to correct the shortcomings of other approaches based on LEFM or cyclic J-integral.

Overall, the numerical results seem in good agreement with the experimental data predicting the fatigue life within errors of 10% in case of SM490 steel and with 20% in case of HT780 steel. The decrease of the accuracy in the predictions of the high strength steel might be due to the choice of the parameters adopted in the simulations.

The main findings can be summarized as follows:

- Higher values of the stress intensity factor are associated with higher rates of the crack growth. In fact, under the same loading conditions and adopting the same material, Model-U is characterized by higher crack growth rates than Model-O, due to the higher amount of plasticization induced.
- The high strength steel showed lower crack growth rates than the SM490 steel adopting the same geometry for the notch. This aspect can be explained once again with the better mechanical performance of the HT780, less prone to plasticize.

- In general, higher values of the stress concentration factor imply lower fatigue life, as experimentally observed in<sup>13)</sup>.
- The difference in fatigue life for the two steels seems to decrease for higher values of the stress concentration factor.
- The numerical comparison between crack initiation and crack propagation life showed that  $N_c$  is higher in all the configurations investigated (i.e., in terms of materials and notch geometry). Higher values of the stress concentration factors are associated with shorter crack initiation lives, as observed in case of Model-U, where the percentage of  $N_c$  can be closer to 50% of the total fatigue life.

Future works will aim to verify the validity of the proposed methodology on different loading conditions and materials.

## REFERENCES

- 1) Paris, P.C. and Erdogan, F. : A critical analysis of crack propagation laws, *Journal of Basic Engineering, Transactions of the ASME, Series D*, Vol. 85, No. 4, pp. 528-34, 1963.
- 2) Gadallah, R., Tsutsumi, S. and Osawa, N. : Numerical investigation on the influence of tensile overload on fatigue life using the interaction integral method, *Journal of Japan Society of Civil Engineers*, Vol. 74, No. 2, pp. I\_137-I\_146, 2018.
- 3) Bai, S., Sha, Y. and Zhang, J. : The effect of compression loading on fatigue crack propagation after a single tensile overload at negative stress ratios, *Int. J. Fatigue*, Vol. 110, pp. 162-171, 2018.
- 4) Bahloul, A. and Bouraoui, C. : The overload effect on the crack-tip cyclic plastic deformation response in SA333 Gr 6 C-Mn steel, *Theor. Appl. Fract. Mec.*, Vol. 99, pp. 27-35, 2019.
- 5) Rice, J.R.: A Path Independent Integral and the Approximate Analysis of Strain Concentration by Notches and Cracks. *J. Appl. Mech.*, Vol. 35, pp. 379-386, 1968.
- 6) Dowling, N. and Begley, J. : Fatigue Crack Growth During Gross Plasticity and the J-Integral, in *Mechanics of Crack Growth*, ed. J. Rice and P. Paris (West Conshohocken, PA: ASTM International), pp. 82-103, 1976.
- 7) Kolednik, O., Schöngrundner, R. and Fischer, F.D. : A new view on J-integrals in elastic-plastic materials, *Int. J. Fract.*, Vol 187, pp. 77-107, 2014.
- 8) Brocks, W. and Scheider, I. : Reliable J-Values - Numerical Aspects of the Path-Dependence of the J-Integral in Incremental Plasticity, *Materials Testing*, Vol. 45, pp. 264-275, 2003.
- 9) Tsutsumi, S. and Fincato, R. : Cyclic plasticity model for fatigue with softening behaviour below macroscopic yielding, *Mater. Design*, Vol. 165, 107573, 2019.
- 10) 堤成一郎, 森田花清 and Fincato, R. : 疲労き裂発生伝播寿命に対する溶接ビード形状の影響に関する解析的検討, *構造工学論文集*, Vol. 63A, pp. 609-618, 2017.
- 11) 平出隆志, 伊木聡, 半田恒久, 田川哲哉, 池田倫生, 森田花清, Fincato, R. and 堤成一郎: 溶接継手疲労寿命に及ぼす熱影響部の繰返し負荷化の材料挙動の影響,

- 溶接学会論文集, Vol. 36, No. 2, pp. 145-151, 2018.
- 12) 堤成一郎, 清川裕樹, Fincato, R., 荻野陽輔, 平田好則 and 浅井知: 溶融池形成および繰返し弾塑性解析を活用した継手の疲労き裂発生寿命評価, *応用力学論文集*, JSCE, Vol. 74, No. 2, pp. 337-347, 2018.
  - 13) Miki, C., Nishimura, T., Tanabe, H. and Nishikawa, K. : Study on estimation of fatigue strengths of notched steel members. *Proc. of the Japan Society of Civil Engineers*. Vol. 1981. No. 316, 1981.
  - 14) 森田 花清, 毛利 雅志, Buherilhan, A., Fincato, R. and 堤成一郎: 鋼材の繰返し弾塑性応答を考慮した溶接継手の疲労き裂発生および伝播寿命評価, *土木学会論文集 A2(応用力学)*, Vol. 76, No. 2, pp. I\_143-I\_152, 2020.
  - 15) 堤成一郎, 長濱 啓和, 清川 裕樹 and Fincato, R. : 局所弾塑性応答に基づく鋼材の疲労亀裂伝播寿命評価 - 応力集中場中存在する表面亀裂の進展特性 -, *土木学会論文集 A2(応用力学)*, Vol. 76, No. 2, pp. I\_399-I\_410, 2020.
  - 16) Tsutsumi, S., Murakami, K., Gotoh, K. and Toyosada, M. : Cyclic plasticity phenomena under macroscopically elastic-high cycle fatigue process, *J. Appl. Mech.*, Vol. 11, pp. 253–261, 2008.
  - 17) Eifler, D. and Macherauch, E. : Microstructure and cyclic deformation behaviour of plain carbon and low-alloyed steels, *Int. J. Fatigue*, Vol. 12, pp. 165–174, 1990.
  - 18) Zhang, J. and Jiang, Y. : An experimental study of inhomogeneous cyclic plastic deformation of 1045 steel under multiaxial cyclic loading, *Int. J. Plast.*, Vol. 21, pp. 2174–2190, 2005.
  - 19) Fincato, R., Tsutsumi, S., Sakai, T. and Terada, K. : 3D crystal plasticity analyses on the role of hard/soft inclusions in the local slip formation, *Int. J. Fatigue*., Vol. 134, 105518, 2020.
  - 20) Fincato, R. and Tsutsumi, S. : An overstress elasto-viscoplasticity model for high/low cyclic strain rates loading conditions: Part I -Formulation and computational aspects, *Int. J. Sol. Struct.*, Vol. 207, pp. 279-294, 2020.
  - 21) Tsutsumi, S., Morita, K., Fincato, R. and Momii H. : Fatigue life assessment of a non-load carrying fillet joint considering the effects of a cyclic plasticity and weld bead shape, *Fracture and Structural Integrity*, Vol. 10, No. 38, pp. 240-250, 2016.
  - 22) Fincato, R. and Tsutsumi, S. : A numerical study of the return mapping application for the subloading surface model, *Engn. Compt.*, Vol. 35, No. 3, pp. 1314-1343, 2018.
  - 23) Iida, K. : Crack initiation life and microfractographic analysis in strain cycling fatigue. *Trans. Japan Weld. Soc.*, Vol. 2, pp. 86–95, 1971.
  - 24) Nieslony, A., Dsoki, C., Kaufmann, H. and Krug, P. : New method for evaluation of the Manson–Coffin–Basquin and Ramberg–Osgood equations with respect to compatibility, *Int. J. Fatigue*, Vol. 30, pp. 1967–77, 2008.
  - 25) Muralidharan, U. and Manson, S.S. : A Modified Universal Slopes Equation for Estimation of Fatigue Characteristics of Metals, *J. Eng. Mater. Technol.*, Vol. 110, pp. 55–8, 1988.
  - 26) 日本材料学会編: 疲労設計便覧, 株式会社養賢堂, 1995.
  - 27) 飯田國廣 and 井上肇: 低サイクル疲労寿命の分布形状に基づいた疲労設計曲線の一考察, *日本造船学会論文集*, Vol. 133, pp. 235-247, 1973.
  - 28) 三木 千壽: 橋梁の疲労と破壊, 朝倉書店, 2011.

(Received June 18, 2021)  
(Accepted November 30, 2021)